(1975).
(2) J. B. Neilands, Ed., "Microbial Iron Metabolism", Academic Press, New York, N.Y., 1974.
(3) J. B. Neilands, "Inorganic Biochemistry", G. Eichhorn, Ed., Elsevier, New York, N.Y., 1973, p 167.
(4) C. E. Lankford, *Crit. Rev. Microbiol.*, **2**, 273 (1973).
(5) J. Leong and K. N. Raymond, *J. Am. Chem. Soc.*, **96**, 1757 (1974).
(6) J. Leong and K. N. Raymond, *J. Am. Chem. Soc.*, **96**, 6628 (1974).
(7) J. Leong, J. B. Neilands, and K. N. Raymond, *Biochem. Biophys. Res. Commun.*, **60**, 1066 (1974).
(8) M. Llinás, *Structure Bond. (Berlin)*, **17**, 135 (1973).
(9) M. Poling and D. Van der Helm, American Crystallographers Association Spring Meeting, Berkeley, Calif., 1974, abstract Q7, p 111.
(10) A. Zalkin, J. D. Forrester, and D. H. Templeton, *J. Am. Chem. Soc.*, **88**, 1810 (1966).
(11) C. I. Brändén, private communication, 1974.
(12) E. Hough and D. Rogers, *Biochem. Biophys. Res. Commun.*, **57**, 73 (1974).
(13) J. R. Pollack and J. B. Neilands, *Biochem. Biophys. Res. Commun.*, **38**, 989 (1970).
(14) I. G. O'Brien and F. Gibson, *Biochim. Biophys. Acta*, **215**, 393 (1970).
(15) J. B. Neilands "Structure and Function of Oxidation Reduction Enzymes", A. Akeson and A. Ehrenberg, Ed., Pergamon Press, Oxford, 1972, pp 541–547.
(16) R. Weinland and E. Walter, *Z. Anorg. Allg. Chem.*, **126**, 141 (1923).
(17) The only triscatechol complex previously resolved is the K[As(catechol)$_3$] salt: A. Rosenheim and W. Plato, *Chem. Ber.*, **58**, 2000 (1925).
(18) J. A. Broomhead, F. P. Dwyer, and J. W. Hogarth, *Inorg. Synth.*, **6**, 183 (1960); F. Galsbok, *ibid.*, **12**, 274 (1970).
(19) G. W. Haupt, *J. Res. Nat. Bur. Stand.*, **48**, 414 (1952).
(20) The ease of oxidizability of coordinated catechol and related ligands has been demonstrated for a series of metal complexes (Ni^{2+}, Cu^{2+}, Zn^{2+}, etc.) by Holm et al. in relation to the 1,2-benzenedithiolato analogues. F. Röhrscheid, A. L. Balch, and R. H. Holm, *Inorg. Chem.*, **5**, 1542 (1966).
(21) J. H. Craddock and M. M. Jones, *J. Am. Chem. Soc.*, **83**, 2839 (1961); **84**, 1098 (1962).
(22) R. D. Gillard and P. R. Mitchell, *Structure Bond. (Berlin)*, **7**, 47 (1970).
(23) C. J. Hawkins, "Absolute Configuration of Metal Complexes", Wiley-Interscience, New York, N.Y., 1971.
(24) K. N. Raymond, S. S. Isied, L. D. Brown, J. H. Nibert, and F. R. Fronczek, following paper.
(25) M. Llinas, D. M. Wilson, and J. B. Neilands, *Biochemistry*, **12**, 3836 (1973).

Coordination Isomers of Biological Iron Transport Compounds. VI. Models of the Enterobactin Coordination Site. A Crystal Field Effect in the Structure of Potassium Tris(catecholato)chromate(III) and -ferrate(III) Sesquihydrates, $K_3[M(O_2C_6H_4)_3]\cdot 1.5H_2O$, M = Cr, Fe[1]

Kenneth N. Raymond,* Stephan S. Isied, Leo D. Brown, Frank R. Fronczek, and J. Hunter Nibert

Contribution from the Department of Chemistry, University of California, Berkeley, California 94720. *Received June 6, 1975*

Abstract: The structures of the title compounds, $K_3[M(cat)_3]\cdot 1.5H_2O$, M = Cr, Fe, have been determined by single-crystal x-ray diffraction methods using counter data. These isostructural tris(catechol) complexes appear to be similar to the coordination sites of the ferric and chromic complexes of the microbial iron transport compound enterobactin (the cyclic triester of 2,3-dihydroxy-*N*-benzoyl-*l*-serine), which is itself a tricatechol. The complexes have approximate molecular D_3 point symmetry, the primary distortion being a bending of the catechol rings away from coplanarity with the O–M–O planes. The average M–O bond lengths are 1.986 (4) Å for Cr and 2.015 (6) Å for Fe. The average ring O–M–O bond angles are 83.56 (14)° for Cr and 81.26 (7)° for Fe. The structural parameters are compared with the $[P(cat)_3]^-$, $[Si(cat)_3]^{2-}$, and $[As(cat)_3]^-$ complexes. A significant increase in the trigonal twist angle of the chromic complex (50.5°) relative to the ferric complex (44.7°) is attributed to a crystal field effect. Dark green crystals of the chromic salt, obtained from basic aqueous solution conform to space group $C2/c$ with a = 20.796 (4), b = 15.847 (4), and c = 12.273 (3) Å with β = 91.84 (1)°. For eight molecules per unit cell the calculated density is 1.68 g/cm^3; the observed density is 1.69 g/cm^3. For 2315 independent data with $F_o^2 > 3\sigma(F_o^2)$ full-matrix least-squares refinement with anisotropic thermal parameters for all nonhydrogen atoms converged to unweighted and weighted R factors of 3.5 and 4.6%, respectively. The ferric compound was prepared from ferric oxide and catechol in excess aqueous base. Dark red-brown crystals of the ferric salt, obtained from basic aqueous solution, conform to space group $C2/c$ with a = 20.612 (7), b = 15.873 (5), and c = 12.307 (4) Å with β = 91.76 (1)°. For eight molecules per unit cell the calculated density is 1.73 g/cm^3; the observed density is 1.72 g/cm^3. For 1445 independent data with $F_o^2 > 3\sigma(F_o^2)$ full-matrix least-squares refinement with anisotropic thermal parameters for all nonhydrogen atoms converged to unweighted and weighted R factors of 4.6 and 4.7%, respectively.

Enterobactin (the cyclic triester of 2,3-dihydroxy-*N*-benzoyl-*l*-serine) is a microbial iron transport agent produced by true bacteria such as *E. coli* and *S. typhimurium*. We have recently reported the preparation of its chromic complex and the optical activity of this and the related model catechol complex.[1] Like all of the siderochromes, enterobactin is a low-molecular-weight compound which is manufactured by the producing organism to facilitate uptake and transport of ferric ion.[2-4] Unlike the ferrichrome[5] or ferrioxamine[6] complexes which contain hydroxamate functional groups, the chelating groups in enterobactin are catechol (1,2-dihydroxybenzene) moieties.

Catecholate dianion has long been known to form coordination compounds with a variety of transition and non-transition metals.[7] As the free anion and, especially, in complexes, catechol can undergo a series of stepwise oxidations. Several reactions of this type have been reported by Holm et al.[8] Recently complexes of the oxidized ligand tetrachloroquinone have been reported.[9] Although under very acid conditions ferric ion oxidizes catechol,[10] near neutral pH

Table I. Summary of Crystal Data for $K_3[M(O_2C_6H_4)_3]\cdot 1.5H_2O$, M = Cr, Fe

Complex	Cr	Fe
Molecular weight, g/mol	520.6	524.5
Space group	*C2/c*	*C2/c*
Cell constants[a]		
a, Å	20.796 (4)	20.612 (7)
b, Å	15.847 (4)	15.873 (5)
c, Å	12.273 (3)	12.307 (4)
β, deg	91.84 (1)	91.76 (1)
Cell volume	4042.5	4024.5
Formula units/cell	8	8
Calcd density, g/cm^3	1.68	1.73
Obsd density, g/cm^3	1.69	1.72
Crystal dimensions, mm	0.35 × 0.18 × 0.17	0.18 × 0.16 × 0.17
Linear absorption, cm^{-1} Coefficient, $\mu_{MoK\alpha}$	12.2	14.2

[a] Ambient temperature of 23°. Mo $K\alpha_1$ radiation, λ 0.70926 Å.

and higher the large formation constant of the catecholate complex reverses the potential for this reaction, and salts of the $[Fe(cat)_3]^{3-}$ (cat = catechol dianion) complex can be isolated.[11] These appear to be analogous to the enterobactin ferric complex, which is known to contain high-spin Fe(III).[1,2] Although the coordination of ferric ion by enterobactin has been assumed to be an octahedral complex which involves only the catechol moieties of the ligand, no firm structural evidence for this has been available.

Also of interest is a comparison of the structural parameters of the ferric and chromic tris(catechol) complexes. High-spin Fe(III) and Cr(III) are within 0.03 Å in ionic radius of one another.[12] The use of Cr(III) in place of Fe(III) to enable transport studies of optically active siderochrome complexes has been justified[5] on the basis that such complexes would be isostructural. However, the crystal field stabilization energy (CFSE) for the chromic complex (12 *Dq*) is considerably greater than that for high spin ferric ion (0 *Dq*). Any shift by the chromic complex towards octahedral from trigonal prismatic coordination, as evidenced by the trigonal twist angle, may be attributed to this crystal field effect.

To determine the coordination geometries of these complexes, and hence indirectly of enterobactin itself, and to explore the crystal field effect of chromic ion on this geometry, we report here the single-crystal structure analyses of the complexes $K_3[M(cat)_3]\cdot 1.5H_2O$, M = Cr, Fe.

Experimental Section

Preparation and Crystallization. Pure, anhydrous ferric oxide (Fe_2O_3, Mallinckrodt), reagent grade catechol ($C_6H_6O_2$, Crown Zellerbach), and potassium hydroxide pellets (85% KOH, Mallinckrodt) were used as supplied. All solvents were degassed before use. Microanalyses were performed by the Microanalytical Laboratory, Department of Chemistry, University of California, Berkeley.

All preparations and handling of the compound were carried out under an oxygen-free nitrogen atmosphere using glass Schlenk apparatus. Ferric oxide (0.80 g, 0.005 mol), catechol (5.5 g, 0.05 mol), and excess KOH (5.7 g, 0.105 mol) were dissolved in 30 ml of H_2O. The resulting red suspension was warmed with stirring for a few hours. The dark red-brown $[Fe(cat)_3]^{3-}$ solution was filtered, leaving no Fe_2O_3 residue, into 60 ml of 95% ethanol. This solution was cooled to −10 °C to effect precipitation. The resulting solid was filtered and washed with EtOH followed by Et_2O and dried in vacuo. The mother liquor may be concentrated to dryness, and this solid washed and combined with the first product, yielding 5 g, 95% yield, of dark red-brown microcrystalline powder. The solid is stable to oxygen but is slightly hygroscopic and the following analysis is for the damp solid. Anal. For $K_3FeC_{18}H_{12}O_6$ + 2.4 waters of hydration, mol wt = 540.39, calcd: C, 39.97; H, 3.13; Fe, 10.34. Obsd: C, 39.93; H, 2.62; Fe, 10.35.

The $[Cr(cat)_3]^{3-}$ complex was prepared as described earlier.[1] Dark green crystals of the chromic sesquihydrate were obtained by slow evaporation of a concentrated solution of the potassium salt in 0.01 M aqueous KOH in a desiccator under nitrogen atmosphere over P_2O_5. Crystals of the ferric complex were obtained by the same procedure from a more basic solution.

Table II. Positional and Thermal Parameters (×10^4) for the Nonhydrogen Atoms in $K_3[Cr(catechol)_3]\cdot 1.5H_2O$

	x	*y*	*z*	β_{11}[a]	β_{22}	β_{33}	β_{12}	β_{13}	β_{23}
Cr	0.32377 (3)[b]	0.01678 (4)	0.10384 (5)	12.96 (17)	27.1 (3)	29.1 (5)	0.26 (18)	3.07 (21)	−1.7 (3)
K_1	0.07046 (5)	0.41615 (7)	0.11938 (8)	18.21 (26)	38.8 (5)	48.5 (8)	−0.6 (3)	7.0 (3)	4.9 (5)
K_2	0.30927 (5)	0.13642 (7)	0.36198 (8)	23.9 (3)	34.5 (5)	41.0 (7)	0.4 (3)	5.3 (4)	1.8 (5)
K_3	0.26236 (5)	0.41057 (7)	0.15856 (8)	19.52 (28)	52.5 (6)	46.3 (8)	3.7 (3)	−2.6 (4)	−12.4 (6)
O_{W1}[c]	0	0.51466 (26)	1/4	16.8 (11)	31.6 (20)	71 (4)	0	1.9 (16)	0
O_{W2}	0.2710 (3)	0.2971 (3)	0.3505 (5)	76.5 (25)	58.5 (27)	227 (8)	29.5 (21)	−39 (4)	−39 (4)
O_1	0.31872 (13)	0.11614 (17)	0.00663 (21)	17.4 (8)	28.6 (13)	31.9 (20)	2.0 (8)	−3.2 (10)	−0.5 (14)
O_2	0.38930 (13)	−0.03418 (17)	0.01146 (22)	17.2 (8)	28.2 (14)	36.2 (21)	2.0 (8)	8.5 (10)	3.6 (14)
O_3	0.25473 (13)	−0.04134 (18)	0.01669 (23)	14.4 (8)	37.1 (15)	47.7 (23)	−1.0 (8)	5.3 (10)	−14.5 (15)
O_4	0.25171 (13)	0.05293 (18)	0.19522 (22)	13.1 (8)	35.1 (14)	37.2 (21)	1.2 (8)	0.5 (10)	−9.2 (14)
O_5	0.38442 (12)	0.08933 (17)	0.19086 (21)	13.6 (7)	28.1 (14)	33.1 (20)	−1.0 (8)	−1.3 (9)	3.1 (13)
O_6	0.34135 (13)	−0.08414 (18)	0.19774 (22)	19.4 (8)	29.7 (13)	38.4 (21)	2.4 (9)	10.6 (10)	3.3 (14)
C_{11}	0.34835 (19)	0.18329 (27)	0.0528 (3)	13.8 (10)	27.8 (20)	29.6 (29)	3.3 (12)	4.6 (14)	−2.9 (20)
C_{12}	0.38391 (18)	0.16896 (26)	0.1513 (3)	10.5 (10)	27.7 (20)	37 (3)	2.5 (12)	4.6 (14)	−0.6 (21)
C_{13}	0.41603 (20)	0.23563 (29)	0.2024 (4)	15.0 (11)	34.1 (23)	50 (4)	−0.9 (13)	1.1 (16)	−2.3 (23)
C_{14}	0.41402 (22)	0.31628 (29)	0.1563 (4)	19.0 (13)	29.3 (23)	69 (4)	−2.5 (13)	8.6 (19)	−9.5 (25)
C_{15}	0.38043 (23)	0.32965 (28)	0.0593 (4)	20.4 (13)	28.1 (21)	64 (4)	4.2 (14)	12.0 (18)	5.8 (24)
C_{16}	0.34708 (21)	0.26392 (28)	0.0082 (3)	18.7 (12)	31.6 (22)	42 (3)	5.2 (13)	3.8 (16)	3.5 (23)
C_{21}	0.40877 (19)	−0.10913 (26)	0.0506 (3)	12.2 (10)	27.6 (20)	40 (3)	1.8 (11)	0.3 (14)	5.1 (20)
C_{22}	0.38276 (20)	−0.13714 (22)	0.1496 (3)	15.5 (12)	26.8 (20)	37 (3)	2.1 (12)	2.7 (15)	2.7 (21)
C_{23}	0.40054 (24)	−0.21508 (29)	0.1910 (4)	26.8 (15)	28.0 (23)	46 (3)	2.2 (14)	2.0 (18)	−2.2 (23)
C_{24}	0.44404 (25)	−0.26553 (24)	0.1366 (4)	27.4 (15)	23.1 (22)	76 (4)	−3.9 (15)	−4.2 (21)	4.9 (25)
C_{25}	0.47013 (22)	−0.2387 (3)	0.0416 (4)	17.8 (12)	37.6 (24)	72 (4)	−5.8 (14)	4.1 (19)	15.9 (27)
C_{26}	0.45206 (20)	−0.16093 (29)	−0.0021 (4)	14.4 (11)	37.4 (23)	49 (3)	1.4 (13)	6.6 (16)	6.3 (23)
C_{31}	0.19646 (20)	−0.02602 (26)	0.0590 (3)	15.0 (11)	28.6 (20)	33 (3)	−1.0 (12)	3.6 (14)	2.7 (20)
C_{32}	0.19517 (20)	0.02608 (26)	0.1513 (3)	15.6 (11)	26.2 (20)	33 (3)	1.8 (12)	0.5 (14)	5.3 (20)
C_{33}	0.13636 (22)	0.0450 (3)	0.1952 (4)	16.6 (12)	40.7 (23)	45 (3)	4.3 (14)	5.6 (16)	−0.1 (23)
C_{34}	0.07995 (22)	0.0108 (3)	0.1495 (4)	14.2 (13)	52.6 (27)	70 (4)	2.0 (15)	9.6 (18)	9.9 (29)
C_{35}	0.08145 (22)	−0.0421 (3)	0.0615 (4)	15.0 (13)	45.4 (26)	70 (4)	−4.8 (14)	−2.1 (18)	10.2 (27)
C_{36}	0.13973 (22)	−0.06008 (29)	0.0156 (4)	18.0 (13)	35.4 (23)	55 (4)	−5.6 (14)	−8 (17)	−1.7 (23)

[a] The form of the anisotropic thermal ellipsoid is $\exp[-(\beta_{11}h^2 + \beta_{22}k^2 + \beta_{33}l^2 + 2\beta_{12}hk + 2\beta_{13}hl + 2\beta_{23}kl)]$. [b] Standard deviations of the least significant figures are given here and elsewhere in parentheses. [c] Located on the crystallographic twofold axis at 0, *y*, ¼.

Table III. Positional Parameters for the Fixed Hydrogen Atoms[a]

Atom	x		y		z	
	Cr	Fe	Cr	Fe	Cr	Fe
H_{13}	0.4410	0.4337	0.2255	0.2374	0.2703	0.2748
H_{14}	0.4362	0.4322	0.3638	0.3686	0.1927	0.1873
H_{15}	0.3803	0.3801	0.3854	0.3859	0.0268	0.0202
H_{16}	0.3221	0.3261	0.2744	0.2740	−0.0592	−0.0608
H_{23}	0.3834	0.3920	−0.2346	−0.2310	0.2583	0.2628
H_{24}	0.4574	0.4586	−0.3203	−0.3290	0.1670	0.1637
H_{25}	0.5002	0.4977	−0.2727	−0.2782	0.0042	0.0011
H_{26}	0.4690	0.4655	−0.1414	−0.1489	−0.0707	−0.0751
H_{33}	0.1342	0.1312	0.0832	0.0753	0.2574	0.2616
H_{34}	0.0395	0.0369	0.0245	0.0207	0.1810	0.1785
H_{35}	0.0417	0.0411	−0.0665	−0.0662	0.0330	0.0315
H_{36}	0.1415	0.1405	−0.0974	−0.0968	−0.0485	−0.0438

[a] The subscript of each hydrogen atom is chosen to be the same as the carbon atom to which it is bonded. The isotropic temperature factor for all the hydrogen atoms is 4.0 Å^2.

Table IV. Root-Mean-Square Amplitude of Vibration along Principal Axes (Å)

Atom	Axis 1		Axis 2		Axis 3	
	Cr	Fe	Cr	Fe	Cr	Fe
M	0.1434 (12)	0.1424 (27)	0.1720 (11)	0.1800 (21)	0.1862 (11)	0.1998 (20)
K_1	0.1711 (16)	0.172 (4)	0.2125 (15)	0.216 (3)	0.2265 (15)	0.2355 (3)
K_2	0.1720 (16)	0.177 (4)	0.2096 (15)	0.224 (3)	0.2315 (15)	0.245 (3)
K_3	0.1753 (17)	0.183 (4)	0.2037 (15)	0.212 (3)	0.2701 (15)	0.295 (3)
O_{W1}	0.192 (7)	0.179 (14)	0.201 (6)	0.202 (13)	0.233 (6)	0.224 (14)
O_{W2}	0.226 (6)	0.262 (13)	0.342 (7)	0.374 (14)	0.501 (8)	0.560 (15)
O_1	0.151 (5)	0.150 (13)	0.186 (4)	0.177 (10)	0.205 (4)	0.212 (9)
O_2	0.145 (5)	0.144 (12)	0.184 (5)	0.185 (10)	0.214 (4)	0.220 (10)
O_3	0.155 (5)	0.153 (12)	0.181 (5)	0.172 (11)	0.240 (4)	0.275 (9)
O_4	0.156 (5)	0.152 (13)	0.169 (5)	0.176 (10)	0.221 (4)	0.216 (9)
O_5	0.154 (5)	0.143 (12)	0.173 (5)	0.173 (10)	0.193 (5)	0.195 (10)
O_6	0.146 (5)	0.146 (13)	0.190 (5)	0.184 (10)	0.227 (4)	0.234 (9)
C_{11}	0.135 (8)	0.130 (20)	0.176 (7)	0.172 (17)	0.197 (7)	0.191 (18)
C_{12}	0.137 (8)	0.116 (22)	0.175 (7)	0.155 (18)	0.191 (7)	0.219 (15)
C_{13}	0.181 (7)	0.166 (19)	0.193 (7)	0.200 (17)	0.211 (7)	0.228 (15)
C_{14}	0.181 (8)	0.173 (17)	0.190 (7)	0.197 (17)	0.249 (7)	0.263 (17)
C_{15}	0.176 (7)	0.170 (18)	0.184 (7)	0.202 (18)	0.251 (7)	0.267 (15)
C_{16}	0.175 (7)	0.166 (20)	0.187 (7)	0.184 (15)	0.225 (7)	0.216 (14)
C_{21}	0.157 (7)	0.143 (17)	0.170 (7)	0.164 (19)	0.197 (7)	0.209 (16)
C_{22}	0.164 (7)	0.167 (19)	0.175 (7)	0.187 (16)	0.197 (7)	0.212 (15)
C_{23}	0.181 (8)	0.168 (21)	0.193 (7)	0.200 (17)	0.244 (7)	0.267 (14)
C_{24}	0.166 (8)	0.187 (18)	0.228 (7)	0.212 (20)	0.261 (7)	0.284 (16)
C_{25}	0.163 (8)	0.161 (18)	0.217 (7)	0.209 (17)	0.261 (7)	0.299 (17)
C_{26}	0.162 (7)	0.160 (20)	0.195 (7)	0.199 (16)	0.228 (7)	0.253 (14)
C_{31}	0.151 (7)	0.136 (20)	0.185 (7)	0.188 (17)	0.193 (7)	0.219 (14)
C_{32}	0.150 (8)	0.157 (18)	0.181 (7)	0.194 (15)	0.194 (7)	0.198 (16)
C_{33}	0.167 (7)	0.146 (21)	0.199 (7)	0.196 (15)	0.234 (7)	0.264 (14)
C_{34}	0.162 (8)	0.166 (17)	0.225 (7)	0.219 (16)	0.271 (7)	0.294 (16)
C_{35}	0.175 (8)	0.172 (19)	0.214 (7)	0.203 (17)	0.262 (7)	0.278 (15)
C_{36}	0.178 (8)	0.183 (16)	0.206 (7)	0.193 (18)	0.228 (7)	0.231 (15)

Unit Cell and Diffraction Data. Precession and Weissenberg photographs for the compounds showed monoclinic symmetry and systematic absences consistent with the space groups Cc or $C2/c$. The latter is confirmed by the solution and successful refinement of the crystal structure. Crystal data, obtained by a least-squares fit to the setting angles of 12 high-angle reflections, are in Table I.

Intensity data were collected on a Picker FACS-1 four-circle diffractometer using monochromatic Mo Kα radiation.[13-15] The data were processed as described previously[16,17] with a parameter, p, introduced to prevent overweighting strong reflections, chosen as 0.04. Absorption effects were judged to be insignificant. The crystal densities were determined by the flotation technique in CH_2Br_2-toluene solutions. The measured densities are 1.69 and 1.72, those calculated for eight formula units per cell are 1.68 and 1.73 g/cm^3 for the chromic and ferric complexes, respectively.

Solution and Refinement of the Structures. Chromium. The presence of four nearly equal heavy atoms and overlapping peaks in the Patterson map led to the use of direct methods via the program MULTAN.[13] From the E map with the highest figure of merit the locations of the heavy atoms and the six catechol oxygen atoms were determined. The remainder of the structure was determined and refined using standard difference Fourier and least-squares techniques. Full-matrix refinements were carried out using the 2315 reflections with $F_o^2 > 3\sigma(F_o^2)$.[18-21] The hydrogen atoms of the catechol rings were found in difference Fourier maps but were put in as fixed atoms such that the C-H bond bisects the C-C-C angle of the ring. The C-H bond length was fixed at 0.95 Å and the isotropic temperature factor was set as 4.0 Å^2. Although the largest peaks in the final difference Fourier (0.35 electron/Å^3 = 7% of a carbon atom) were around the water oxygen atoms, the water hydrogen atoms could not be located. The water molecules show a large amount of apparent thermal motion. The final unweighted (R_1) and weighted (R_2) agreement factors are 3.5 and 4.6%, respectively,[22] and the error in an observation of unit weight is 1.59. Table II gives the positional and thermal parameters of the nonhydrogen atoms. Table III gives the final positional parameters for the fixed hydrogen atoms and Table IV lists the amplitudes of vibration derived from the thermal parameters.[23]

Iron. Weissenberg photographs revealed that the unit cells of the compounds are nearly identical. Structure factors based upon refined positional and thermal parameters from the Cr structure afforded an R factor of 15% when compared to the Fe data. Catechol hydrogen atoms were included as described above. The largest peaks in the final difference Fourier were 0.25 electron/Å^3. The

Table V. Positional and Thermal Parameters ($\times 10^4$) for the Nonhydrogen Atoms in $K_3[Fe(catechol)_3] \cdot 1.5H_2O$

	x	y	z	β_{11}[a]	β_{22}	β_{33}	β_{12}	β_{13}	β_{23}
Fe	0.32558 (6)[b]	0.01842 (8)	0.10584 (11)	14.9 (3)	31.0 (6)	27.6 (10)	−0.2 (4)	2.5 (5)	−2.3 (7)
K_1	0.06608 (9)	0.41838 (12)	0.11675 (17)	19.6 (6)	43.0 (11)	45.4 (19)	−1.4 (7)	6.7 (9)	3.0 (12)
K_2	0.30668 (10)	0.13637 (13)	0.36373 (18)	26.8 (7)	40.5 (11)	42.7 (19)	2.1 (7)	4.8 (9)	3.0 (12)
K_3	0.25936 (10)	0.40707 (15)	0.15749 (18)	22.1 (7)	60.8 (14)	51.4 (21)	6.0 (7)	−4.0 (9)	−15.6 (13)
O_{W1}[c]	0	0.5208 (5)	1/4	15.8 (21)	32 (4)	63 (8)	0	5 (4)	0
O_{W2}	0.2651 (5)	0.2958 (5)	0.3558 (10)	92 (5)	80 (6)	284 (19)	40 (4)	−54 (8)	−41 (9)
O_1	0.32399 (25)	0.1185 (3)	0.0049 (5)	18.2 (18)	29 (3)	30 (5)	3.9 (17)	−0.5 (24)	−0 (3)
O_2	0.38954 (25)	−0.0368 (3)	0.0104 (5)	17.1 (16)	28 (3)	41 (5)	2.5 (17)	10.5 (24)	3 (3)
O_3	0.25394 (26)	−0.0390 (3)	0.0173 (5)	13.1 (17)	48 (4)	56 (6)	−1.8 (19)	3.5 (26)	−22 (3)
O_4	0.25064 (26)	0.0484 (3)	0.1977 (5)	14.7 (17)	35 (3)	32 (5)	1.9 (16)	−0.1 (24)	−6 (3)
O_5	0.38376 (24)	0.0965 (3)	0.1941 (5)	14.0 (16)	27.1 (29)	30 (5)	2.6 (17)	−0.9 (22)	5 (3)
O_6	0.34841 (27)	−0.0825 (3)	0.2016 (5)	22.4 (18)	27 (3)	36 (5)	2.3 (19)	10.4 (25)	4 (3)
C_{11}	0.3516 (4)	0.1866 (5)	0.0518 (8)	10.9 (24)	23 (5)	40 (8)	1.3 (26)	7 (4)	−1 (5)
C_{12}	0.3842 (4)	0.1748 (6)	0.1528 (7)	10.0 (24)	32 (5)	30 (8)	6.9 (27)	−1 (4)	9 (5)
C_{13}	0.4133 (4)	0.2434 (6)	0.2043 (8)	17.3 (28)	37 (5)	45 (9)	−5 (3)	−3 (4)	−5 (5)
C_{14}	0.4115 (5)	0.3217 (6)	0.1532 (9)	21 (3)	31 (5)	69 (12)	−6 (3)	8 (5)	−14 (6)
C_{15}	0.3802 (5)	0.3325 (6)	0.0545 (9)	27 (3)	30 (5)	58 (11)	8 (3)	8 (5)	10 (6)
C_{16}	0.3494 (4)	0.2657 (6)	0.0061 (8)	17.3 (26)	33 (5)	37 (9)	3.1 (29)	2 (4)	4 (5)
C_{21}	0.4097 (4)	−0.1105 (6)	0.0482 (7)	10.3 (23)	30 (5)	36 (8)	−3.3 (26)	2 (4)	−8 (5)
C_{22}	0.3871 (4)	−0.1371 (6)	0.1507 (8)	19.9 (29)	28 (5)	38 (9)	−2 (3)	−3 (4)	0 (5)
C_{23}	0.4059 (5)	−0.2139 (6)	0.1931 (8)	33 (4)	31 (5)	33 (9)	−2 (3)	2 (5)	3 (5)
C_{24}	0.4467 (5)	−0.2656 (6)	0.1348 (10)	37 (4)	28 (5)	59 (11)	4 (3)	−3 (5)	1 (6)
C_{25}	0.4694 (5)	−0.2423 (7)	0.0385 (10)	18 (3)	38 (6)	91 (13)	11 (3)	−9 (5)	−19 (7)
C_{26}	0.4504 (4)	−0.1646 (6)	−0.0057 (8)	16.2 (28)	46 (5)	44 (9)	−3 (3)	9 (4)	−9 (6)
C_{31}	0.1964 (4)	−0.0255 (5)	0.0600 (8)	20.5 (28)	19 (4)	44 (8)	−6 (3)	−1 (4)	−5 (5)
C_{32}	0.1932 (4)	0.0226 (5)	0.1549 (7)	16.5 (26)	29 (4)	38 (8)	1 (3)	−4 (4)	4 (5)
C_{33}	0.1337 (5)	0.0408 (6)	0.1983 (8)	18.2 (28)	52 (6)	33 (8)	5 (3)	6 (4)	8 (5)
C_{34}	0.0778 (4)	0.0078 (7)	0.1496 (10)	14.4 (27)	57 (7)	77 (11)	3 (3)	9 (5)	18 (7)
C_{35}	0.0799 (5)	−0.0429 (6)	0.0623 (9)	19 (3)	51 (6)	52 (10)	−9 (3)	−7 (5)	8 (6)
C_{36}	0.1390 (5)	−0.0602 (5)	0.0174 (8)	22 (3)	30 (5)	51 (9)	−4 (3)	5 (5)	−5 (5)

[a] The form of the anisotropic thermal ellipsoid is $\exp[-(\beta_{11}h^2 + \beta_{22}k^2 + \beta_{33}l^2 + 2\beta_{12}hk + 2\beta_{13}hl + 2\beta_{23}kl)]$. [b] Standard deviations of the least significant figures are given here and elsewhere in parentheses. [c] Located on the crystallographic twofold at $0, y, \frac{1}{4}$.

water hydrogens were not located. The final unweighted (R_1) and weighted (R_2) agreement factors are 4.6 and 4.7%, respectively,[22] and the error in an observation of unit weight is 1.34. Table V gives the positional and thermal parameters of the nonhydrogen atoms. Table III gives the final positional parameters for the fixed hydrogen atoms and Table IV lists the amplitudes of vibration derived from the thermal parameters.[23]

Description of the Structures

The crystal structure consists of discrete $[M(cat)_3]^{3-}$ anions, potassium cations, and water molecules of crystallization, as shown in Figure 1. The three cations are coordinated by oxygen atoms of the catechol and water molecules. The structure of the anion is shown in Figure 2. The $[M(cat)_3]^{3-}$ complexes are distorted from octahedral geometry with approximately D_3 molecular point symmetry. The average ring O-M-O angles are reduced to 83.56 (14)° for Cr and 81.26 (7)° for Fe (from 90° for an octahedron). The trigonal twist angles of the top trigonal face relative to the bottom are 50.5 (6)° for Cr and 44.7 (10)° for Fe (from 60° for an octahedron).

Average bond lengths and angles for both complexes are shown in Figure 3. Individual bond lengths and angles are presented in Tables VI and VII. The average M-O bond lengths are 1.986 (4) Å for Cr and 2.015 (6) Å for Fe, the difference being about that expected from the metal ionic radii.[12] Both values appear to be slightly larger than those found in similar tris-chelate complexes of Cr(III) and Fe(III). The values of 1.951 (6) Å in $Cr(acac)_3$,[24] 1.965 (2) Å in *fac*-$Cr(glycinato)_3$,[25] and 1.96 (4) Å in $Cr(oxalato)_3$[26] seem systematically smaller than our Cr-O distance. The values of 1.992 (6) Å in $Fe(acac)_3$,[27] 2.008 (3) Å in $Fe(trop)_3$,[28] and 2.00 (1) Å in $Fe(cupferron)_3$[29] (cupferron = *N*-nitrosophenylhydroxylamine) may also be smaller than our Fe-O distance.

The primary distortion of the $[M(cat)_3]^{3-}$ complex from D_3 symmetry is the bending of two of the rings at the oxy-

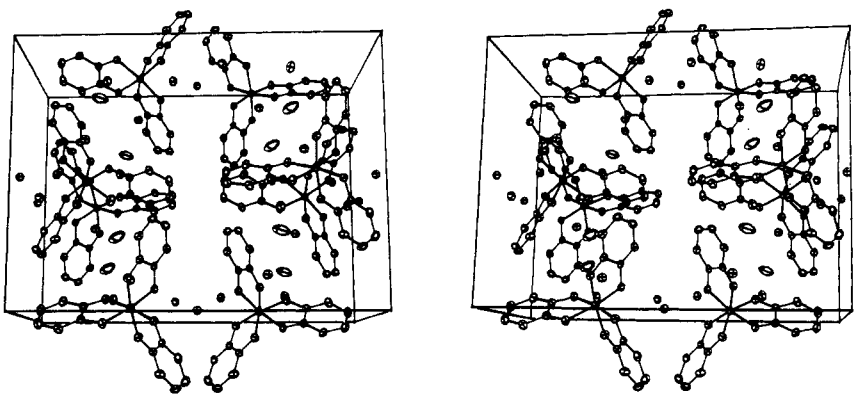

Figure 1. A stereoscopic packing diagram of the $K_3[M(O_2C_6H_4)_3]$, M = Cr, Fe, structures. The vertical axis is b, and a is the horizontal axis. The individual atoms are drawn at 30% probability contours of the thermal motion in the Cr structure.

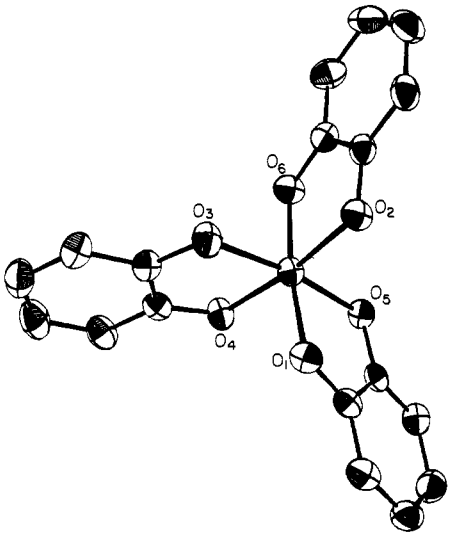

Figure 2. A perspective drawing of the $[M(O_2C_6H_4)_3]^{3-}$ anions, M = Cr, Fe, as viewed down the molecular threefold axis. The catechol ring carbon atoms C_{11}, C_{21}, C_{31} are bound to O_1, O_2, and O_3, respectively, the other carbon atoms $C_{12} \ldots C_{16}$, $C_{22} \ldots C_{26}$, and $C_{32} \ldots C_{36}$ are given increasing numbers in a clockwise fashion. The thermal ellipsoids illustrated are those of the Cr complex and are drawn at the 30% probability level.

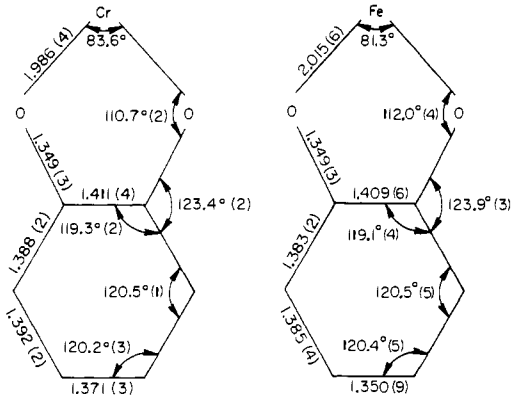

Figure 3. Schematic diagram of the chromic and ferric catecholate coordination geometries, showing the average bond distances and angles.

gen atoms. The dihedral angles between the planes of the catechol rings and the O-Cr-O planes are 8.6, 5.0, and 3.0° for rings one through three, respectively, and 9.2, 6.2, and 4.9°, respectively, between the catechol rings and the O-Fe-O planes. The least-squares planes (Table VIII) show the catechol rings are strictly planar. However, the oxygen atoms deviate from these planes to a small extent and, for rings one and two, both metal atoms are well out of the plane as indicated by the dihedral angles just described. Since ring three does not show the same distortion, there is no apparent intramolecular steric force requiring this distortion and the distortion is nearly the same for both the Cr and Fe structures, the bending is ascribed to the crystal intermolecular forces. It does not appreciably affect the coordination polyhedron.

Discussion

Catechol is a very weak acid (pK_{a_1} = 9.45, pK_{a_2} = 12.89)[30] and hence at low pH is a poor ligand. The kinetics and equilibria of its reactions with ferric ion under acidic conditions have been investigated.[10] Under such conditions, even with excess catechol ferric ion forms only a transient 1:1 complex which eventually undergoes a redox reaction to give ferrous ion and orthoquinone as products. This reaction has a redox potential just greater than zero at pH 1. At higher pH's the extremely large formation constant of the tris(catechol) ferric complex strongly reverses the potential, such that ferrous ion will reduce orthoquinone to form the tris(catechol) ferric complex. In the absence of air, both the chromic and ferric tris(catechol) complexes are stable indefinitely in basic aqueous solution.[1]

The circular dichroism spectra of the tris(catechol)chromic complex, $[Cr(cat)_3]^{3-}$, and the chromic enterobactin complex, $[Cr(ent)]^{3-}$, are so similar as to indicate nearly identical coordination geometries for the chromium ions.[1] The uv-visible spectra of the tris(catechol) ferric complex, $[Fe(cat)_3]^{3-}$, and the ferric enterobactin complex, $[Fe(ent)]^{3-}$, are also nearly identical.[31] Thus the geometries reported here are presumed to be substantially those of the metal binding portion of enterobactin itself in these complexes.

Three other tris(catechol) complexes have been the subjects of structure analysis, Δ-$K[As(cat)_3]\cdot 1.5H_2O$,[32] $[NH(C_2H_5)_3][P(cat)_3]$,[33] and $[C_5H_5NH]_2[Si(cat)_3]$.[34] The structural parameters of the tris(catechol) complexes are compared in Table IX. The ligand bite (ratio of the O-O ring distance to the M-O distance), the trigonal twist angle, and the trigonal plane-to-plane distance vary smoothly across the table. The final geometry represents a balance between distortions of the O-M-O angle and O-O ring distance and variations of the twist angle from octahedral to trigonal prismatic. A detailed analysis of tris-chelate geometries using a simple central force-field potential energy calculation has been presented.[35] Recently a more extensive discussion has appeared which uses a different theoretical model but reaches substantially the same conclusions.[36] It was found that the twist angle was a linear function of the ligand bite, b, for a wide range of tris-chelate complexes. A linear regression analysis of the 19 compounds reported (this excludes the three worst data pairs at low bite distances in Table I of ref 35) gives: twist angle = $-73.95 + 94.10b$. No catechol complexes were included in the compounds discussed previously.[35] However, the calculated and observed twist angles are 60.7 (58.9), 57.4 (55.9), 57.0

Table VI. Bond Distances in $K_3[M(cat)_3]\cdot 1.5H_2O$, M = Cr, Fe

	Distance, Å			Distance, Å	
Atoms	Cr	Fe	Atoms	Cr	Fe
$M-O_1$	1.976 (3)	2.017 (5)	$C_{25}-C_{26}$	1.391 (7)	1.399 (12)
$M-O_2$	1.973 (3)	1.996 (5)	$C_{26}-C_{21}$	1.393 (6)	1.383 (11)
$M-O_3$	1.989 (3)	2.025 (6)			
$M-O_4$	1.985 (3)	2.000 (6)	$C_{31}-C_{32}$	1.403 (6)	1.399 (12)
$M-O_5$	1.992 (3)	2.018 (6)	$C_{32}-C_{33}$	1.385 (6)	1.383 (11)
$M-O_6$	1.998 (3)	2.035 (6)	$C_{33}-C_{34}$	1.394 (7)	1.385 (13)
			$C_{34}-C_{35}$	1.368 (7)	1.344 (13)
O_1-C_{11}	1.346 (5)	1.343 (9)	$C_{35}-C_{36}$	1.383 (6)	1.381 (12)
O_2-C_{21}	1.339 (5)	1.322 (9)	$C_{36}-C_{31}$	1.388 (6)	1.393 (11)
O_3-C_{31}	1.355 (5)	1.330 (9)			
O_4-C_{32}	1.347 (5)	1.345 (9)	K_1-O_1	2.863 (3)	2.815 (6)
O_5-C_{12}	1.352 (5)	1.344 (9)	K_1-O_2	2.620 (3)	2.628 (6)
O_6-C_{22}	1.353 (5)	1.346 (10)	K_1-O_6	2.853 (3)	2.804 (6)
			K_1-O_{W1}	2.703 (3)	2.706 (5)
$C_{11}-C_{12}$	1.414 (6)	1.407 (11)	K_2-O_2	2.927 (3)	2.912 (6)
$C_{12}-C_{13}$	1.389 (6)	1.387 (11)	K_2-O_3	2.702 (3)	2.696 (6)
$C_{13}-C_{14}$	1.398 (6)	1.393 (12)	K_2-O_4	2.686 (3)	2.704 (6)
$C_{14}-C_{15}$	1.377 (7)	1.368 (9)	K_2-O_5	2.761 (3)	2.736 (6)
$C_{15}-C_{16}$	1.390 (7)	1.363 (12)	K_2-O_{W2}	2.670 (5)	2.672 (8)
$C_{16}-C_{11}$	1.390 (6)	1.375 (11)	K_3-O_1	2.629 (3)	2.627 (6)
$C_{21}-C_{22}$	1.417 (6)	1.421 (12)	K_3-O_3	3.000 (3)	3.008 (7)
$C_{22}-C_{23}$	1.381 (6)	1.377 (12)	K_3-O_4	2.903 (3)	2.877 (6)
$C_{23}-C_{24}$	1.393 (7)	1.390 (13)	K_3-O_6	2.831 (3)	2.864 (6)
$C_{24}-C_{25}$	1.369 (7)	1.339 (14)	K_3-O_{W2}	2.964 (6)	3.013 (12)

Table VII. Bond Angles in $K_3[M(cat)_3] \cdot 1.5H_2O$, M = Cr, Fe

Atoms	Angle, deg Cr	Angle, deg Fe	Atoms	Angle, deg Cr	Angle, deg Fe
O_1–M–O_5	83.35 (11)	81.13 (23)	O_4–C_{32}–C_{31}	118.1 (4)	115.5 (8)
O_2–M–O_6	83.50 (12)	81.37 (23)	O_4–C_{32}–C_{33}	123.1 (4)	124.5 (9)
O_3–M–O_4	83.83 (11)	81.29 (22)	O_5–C_{12}–C_{11}	117.0 (4)	116.7 (8)
O_1–M–O_2	90.20 (11)	88.99 (23)	O_5–C_{12}–C_{13}	123.3 (4)	124.1 (8)
O_1–M–O_3	91.20 (12)	91.44 (24)	O_6–C_{22}–C_{21}	116.5 (4)	116.0 (8)
O_1–M–O_4	94.86 (12)	99.34 (22)	O_6–C_{22}–C_{23}	124.2 (4)	123.9 (9)
O_1–M–O_6	172.34 (12)	167.41 (22)			
O_2–M–O_3	90.09 (12)	88.24 (23)	C_{11}–C_{12}–C_{13}	119.6 (4)	119.3 (8)
O_2–M–O_4	172.15 (12)	166.74 (22)	C_{12}–C_{13}–C_{14}	120.3 (4)	119.2 (9)
O_2–M–O_5	96.15 (11)	101.21 (21)	C_{13}–C_{14}–C_{15}	119.9 (4)	121.2 (9)
O_3–M–O_5	171.72 (12)	167.81 (22)	C_{14}–C_{15}–C_{16}	120.4 (4)	119.4 (9)
O_3–M–O_6	93.16 (13)	96.30 (24)	C_{15}–C_{16}–C_{11}	120.6 (4)	121.5 (9)
O_4–M–O_5	90.41 (11)	90.33 (22)	C_{16}–C_{11}–C_{12}	119.1 (4)	119.4 (9)
O_4–M–O_6	91.87 (11)	91.65 (22)	C_{21}–C_{22}–C_{23}	119.4 (4)	120.2 (9)
O_5–M–O_6	92.96 (12)	92.77 (23)	C_{22}–C_{23}–C_{24}	120.5 (4)	119.6 (9)
			C_{23}–C_{24}–C_{25}	120.7 (4)	121.9 (9)
M–O_1–C_{11}	111.2 (2)	111.8 (4)	C_{24}–C_{25}–C_{26}	119.6 (4)	119.1 (9)
M–O_2–C_{21}	111.3 (2)	112.8 (4)	C_{25}–C_{26}–C_{21}	120.9 (4)	121.8 (9)
M–O_3–C_{31}	110.5 (2)	111.1 (4)	C_{26}–C_{21}–C_{22}	118.9 (4)	117.5 (9)
M–O_4–C_{32}	110.3 (2)	113.1 (4)	C_{31}–C_{32}–C_{33}	118.8 (4)	120.0 (9)
M–O_5–C_{12}	110.4 (2)	112.0 (4)	C_{32}–C_{33}–C_{23}	120.1 (4)	119.3 (9)
M–O_6–C_{22}	110.6 (2)	111.5 (4)	C_{33}–C_{34}–C_{35}	121.0 (4)	121.8 (9)
			C_{34}–C_{35}–C_{36}	119.4 (4)	119.3 (9)
O_1–C_{11}–C_{12}	116.9 (4)	117.2 (8)	C_{35}–C_{36}–C_{31}	120.6 (4)	121.4 (9)
O_1–C_{11}–C_{16}	123.9 (4)	123.4 (9)	C_{36}–C_{31}–C_{32}	120.0 (4)	118.0 (9)
O_2–C_{21}–C_{22}	117.8 (4)	117.8 (8)			
O_2–C_{21}–C_{26}	123.3 (4)	124.6 (9)			
O_3–C_{31}–C_{32}	117.1 (4)	118.9 (8)			
O_3–C_{31}–C_{36}	122.9 (4)	123.0 (8)			

Table VIII. Weighted Least-Squares Planes[a] for the Aromatic Rings[b]

Ring 1			Ring 2			Ring 3		
	Deviation, A			Deviation, A			Deviation, A	
Atom	Cr	Fe	Atom	Cr	Fe	Atom	Cr	Fe
C_{11}	−0.004 (4)	0.005 (8)	C_{21}	−0.001 (4)	0.001 (8)	C_{31}	−0.010 (4)	−0.031 (9)
C_{12}	0.007 (4)	0.007 (8)	C_{22}	0.004 (4)	0.000 (8)	C_{32}	0.012 (4)	0.024 (8)
C_{13}	−0.003 (4)	−0.015 (9)	C_{23}	−0.003 (5)	0.002 (9)	C_{33}	−0.005 (5)	−0.002 (9)
C_{14}	−0.006 (4)	0.005 (9)	C_{24}	−0.004 (5)	−0.006 (10)	C_{34}	−0.009 (5)	−0.019 (10)
C_{15}	0.011 (4)	0.014 (9)	C_{25}	0.008 (5)	0.006 (10)	C_{35}	0.011 (5)	0.013 (9)
C_{16}	−0.004 (4)	−0.017 (8)	C_{26}	−0.005 (4)	−0.003 (9)	C_{36}	0.001 (5)	0.015 (9)
O_1	0.018	0.024	O_2	−0.027	−0.021	O_3	−0.028	−0.065
O_5	0.024	0.008	O_6	0.018	0.023	O_4	0.095	0.095
M	−0.202	−0.230	M	−0.132	−0.163	M	0.002	−0.048

A =	17.278	17.716	A =	15.414	16.052	A =	1.731	1.692
B =	−3.395	−3.297	B =	6.813	6.838	B =	−12.579	−12.837
C =	−6.627	−6.069	C =	6.033	5.316	C =	7.358	7.133
D =	5.050	5.295	D =	5.864	6.077	D =	1.111	1.118

Dihedral Angles (deg) between Planes

	Cr	Fe
Ring 1, Ring 2	75.0	68.6
Ring 1, Ring 3	94.0	92.9
Ring 2, Ring 3	88.2	91.1

[a] Equation for the least-squares plane is $Ax + By + Cz - D = 0$. [b] The catechol oxygens and metal are not included in the least-squares plane, only the six ring carbon atoms. Deviations from the plane of the oxygens and the metal are listed.

(55.2), 51.5 (50.5), and 48.7 (44.7) for the P, Si, As, Cr, and Fe catechol complexes, respectively. The calculated catechol twist angles seem to be systematically too high but are generally in agreement with those observed. Since the ligand bite is itself a nearly linear function of the metal ion size, the linear relation between the twist angle and the ligand bite really has its origin in the following; as the metal ion size increases, increasing distortions of the metal-oxygen-catechol ring force the twist angle to decrease.

However, in comparing the chromic and ferric catechol structures, the difference in M-O bond length is not large enough to cause the nearly 6° difference in twist angle, which must be attributed to a difference in electronic configuration. Wentworth has presented a theoretical calculation of the difference in crystal field stabilization energy (ΔCFSE) between octahedral and trigonal prismatic coordinations.[37] His model, which maximizes intraligand bonding interactions and minimizes all nonbonded contacts to find an energy minimum, determines the energies of the d orbitals as a function of the twist angle. From his equations one can estimate the ΔCFSE for conversion of the chromic complex (twist angle = 50.5°) to the ferric complex geometry (twist angle = 44.7°). This value, 0.6 *Dq*, and the spectroscopic value of 1750 cm^{-1} for *Dq* in the similar

Table IX. Structural Parameters for $[M(cat)_3]^{n-}$ Complexes

	Pa	Sib	Asc	Crd	Fed
Average M–O distance (Å)e	1.723 (4)	1.784 (18)	1.843 (5)	1.986 (4)	2.015 (6)
Average ring O–M–O angle (deg)	91.4 (2)	88.7 (2)	88.2 (5)	83.56 (14)	81.26 (7)
Average O–O ring distance (Å)	2.466 (6)	2.490 (6)	2.565 (7)	2.646 (6)	2.625 (2)
Ligand bitef	1.431	1.396	1.392	1.333	1.303
Trigonal twist angle (deg)g	58.9	55.9 (5)	55.2 (10)	50.5 (6)	44.7 (10)
Plane-to-plane distance (Å)h	1.940	2.093	2.194	2.247	2.303

a Reference 33. b Reference 34. c Reference 32. d This work. e The standard deviations in the averages are computed from the variance. f This is the ratio of the O–O ring distance to M–O distance. See ref 37. g This angle is defined by viewing the complex in projection down the molecular threefold axis. It is then the rotation required to bring the top and bottom planes (of three oxygen atoms each) into coincidence. This angle is 60° for octahedral and 0° for trigonal prismatic coordination. h This is the plane-to-plane distance for the two trigonal oxygen atom planes described in footnote g.

$[Cr(ox)_3]^{3-}$ complex[38] give an estimate of 3 kcal difference for ΔCFSE. This would correspond to a bending force constant of 1 mdyn/Å, assuming an harmonic oscillator and a 6° amplitude (= 0.1 rad or 0.2 Å). Although similar angle bending force constants are typically lower than this estimate, they are within this order of magnitude.[39] Thus the calculated change in CFSE is sufficiently large to account for the difference in twist angles of the Cr and Fe complexes.

One final comment can be made on a related structure. The recent report of the dimeric tris-complex $Mo_2(O_2C_6Cl_4)_6$[40] interpreted the short intrachelate ring O–O distance of 2.43 and O–Mo–O angle of 78° as due to intra-ring O–O bonding interactions. It is clear from the trend observed in the structural parameters given in Table IX that this bonding does not have to be involved to explain the $Mo_2(O_2C_6Cl_4)_6$ structure. Two conclusions do emerge: (1) from structural parameters the complex can be formally characterized as a tetrachlorocatechol complex of the Mo(VI) ion (of course there must be extensive electron delocalization in the complex) and (2) the Mo–O bond length of 1.94 Å for the chelate rings when compared with the structural data in Table IX leads to an expected O–Mo–O bond angle of 80–85°. In all of the octahedral tris(catechol) complexes, the geometries distort to distribute the strain induced by the conflicting geometrical requirements of octahedral coordination, fixed metal-oxygen distances and the structural parameters of the ligand. For the nonbridging chelate ligand this strain lowers the O–Mo–O bond angle and diminishes the O–O nonbonded distance. For the bridging ligand the reverse is true. This explains the different structural parameters observed for the bridging and chelate rings in $Mo_2(O_2C_6Cl_4)_6$.[40]

Acknowledgment. This research is supported by the National Institutes of Health through Grant AI 11744. Funds for instrumental facilities have been provided by the National Science Foundation through grants GP 10510 and GP 36977X. The authors wish to acknowledge the experimental assistance of Mr. Ted Baker and Ms. Ninon Kafka.

Supplementary Material Available: structure factor amplitudes (27 pages). Ordering information is given on any current masthead page.

References and Notes

(1) Part V: S. Isied, G. Kuo, and K. N. Raymond, *J. Am. Chem. Soc.*, preceding paper in this issue.
(2) J. B. Neilands, Ed., "Microbial Iron Metabolism", Academic Press, New York, N.Y., 1974.
(3) J. B. Neilands, "Inorganic Biochemistry", G. Eichhorn, Ed., Elsevier, New York, N.Y., 1973, p 167.
(4) C. E. Lankford, *Crit. Rev. Microbiol.*, **2**, 273 (1973).
(5) J. Leong, J. B. Neilands, and K. N. Raymond, *Biochem. Biophys. Res. Commun.*, **60**, 1066 (1974).
(6) J. Leong and K. N. Raymond, *J. Am. Chem. Soc.*, **97**, 293 (1975).
(7) *Beilstein*, Band VI, E I 378, E II 771, E III 4195.
(8) F. Rohrscheid, A. L. Balch, and R. H. Holm, *Inorg. Chem.*, **5**, 1542 (1966).
(9) (a) C. G. Pierpont, H. H. Downs, and T. G. Rukavina, *J. Am. Chem. Soc.*, **96**, 5573 (1974); (b) H. H. Downs and C. G. Pierpont, Abstracts, 169th National Meeting of the American Chemical Society, Inorg. Div., No. 29, Philadelphia, Pa., 1975.
(10) E. Mentasti, E. Pelizzetti, and G. Saini, *J. Chem. Soc., Dalton Trans.*, 2605, 2609 (1973).
(11) R. Weinland and K. Binder, *Ber. Dtsch. Chem. Ges.*, **45**, 148 (1912).
(12) R. D. Shannon and C. T. Prewitt, *Acta Crystallogr., Sect. B*, **25**, 925 (1969).
(13) The programs used for the PDP8/E computer were those written by Busing and Levy, as modified by Picker Corp. In addition to local programs for the U.C. Berkeley CDC 6400 and the Lawrence Berkeley Laboratory CDC 7600 computers, the following programs or modifications were used: Zalkin's FORDAP Fourier program; Ibers' NUCLS, a group least-squares version of the Busing–Levy ORFLS program; ORFFE, a function and error program by Busing and Levy; Johnson's ORTEP, a thermal ellipsoid plot program; FAME, a structure factor normalization program by Dewar; and MULTAN, a direct methods program by Main, Woolfson, and Germain.
(14) Each data crystal was mounted on the tip of a glass rod along the needle (*a*) axis. The crystals gave ω scan widths at half-height of approximately 0.07–0.09° for several low-angle reflections. The data were collected in the θ–2θ scan mode with a scan rate of 1°/min from 0.65° below the $K\alpha_1$ peak to 0.65° above the $K\alpha_2$ peak. Stationary-crystal stationary-counter background counts of 10 s each were taken at the start and end of each scan (ref 15). Intensity data for the unique form $\pm h, +k, +l$ were collected to a 2θ angle of 48° for the chromic salt and 50° for the ferric salt. During the chromic compound data collection the intensities of the 600, 020, and 004 reflections were measured as standards after every 80 reflections. During the ferric compound data collection the intensities of the 12·0·0, 020, and 004 reflections were measured as standards after every 100 reflections. The standards showed only a small random 1–2% deviation during the course of each experiment.
(15) Copper foil attenuators were automatically inserted if the counting rate approached 10^4 counts/sec. The takeoff angle for the x-ray tube was 2° and the Bragg 2θ angle for the graphite monochromator was 12.16°. The detector was located 32 cm from the source and had a 7 × 7 mm receiving aperature. The pulse-height analyzer was set to a 95% window centered on the Mo Kα peak.
(16) E. C. Baker, L. D. Brown, and K. N. Raymond, *Inorg. Chem.*, **14**, 1376 (1975).
(17) E. N. Duesler and K. N. Raymond, *Inorg. Chem.*, **10**, 1486 (1971).
(18) In all refinements the function minimized was $\sum w(|F_o| - |F_c|)^2$, where F_o and F_c are the observed and calculated structure factors. The weighting factor, w, is $4F_o^2/\sigma^2(F_o^2)$. The atomic scattering factors for the nonhydrogen atoms were taken from the tabulations of Cromer and Mann (ref 19). Hydrogen scattering factor values were those calculated by Stewart, Davidson, and Simpson (ref 20). Corrections for anomalous dispersion effects for the metal and K were made using the $\Delta f'$ and $\Delta f''$ values of Cromer (ref 21).
(19) D. T. Cromer and B. Mann, *Acta Crystallogr., Sect. A*, **24**, 321 (1968).
(20) R. F. Stewart, E. R. Davidson, and W. T. Simpson, *J. Chem. Phys.*, **42**, 3175 (1965).
(21) D. T. Cromer, *Acta Crystallogr.*, **18**, 17 (1965).
(22) $R_1 = \sum||F_o| - |F_c||/\sum|F_o|$; $R_2 = [\sum w(|F_o| - |F_c|)^2/\sum w|F_o|^2]^{1/2}$. The error in an observation of unit weight is defined as $[\sum w(|F_{obsd}| - |F_{calcd}|)^2/(N_{obsd} - N_{var})]^{1/2}$.
(23) See paragraph at end of paper for supplementary material.
(24) B. Morosin, *Acta Crystallogr.*, **19**, 131 (1965).
(25) R. F. Bryan, P. T. Greene, P. F. Stokely, and E. W. Wilson, Jr., *Inorg. Chem.*, **10**, 1468 (1971).
(26) J. N. van Niekerk and F. R. L. Schoening, *Acta Crystallogr.*, **5**, 499 (1952).
(27) J. Iball and C. H. Morgan, *Acta Crystallogr.*, **23**, 239 (1967).
(28) T. A. Hamor and D. J. Watkin, *Chem. Commun.*, 440 (1969).
(29) D. van der Helm, K. L. Merritt, Jr., R. Degeilh, and C. H. MacGillavry, *Acta Crystallogr.*, **18**, 355 (1965).
(30) C. F. Timberlake, *J. Chem. Soc.*, 4987 (1957).
(31) To be submitted for publication.
(32) A. Kobayashi, T. Ito, F. Marumo, and Y. Sacto, *Acta Crystallogr., Sect. B*, **28**, 3446 (1972).

(33) H. R. Allcock and E. C. Bissell, *J. Am. Chem. Soc.*, **95**, 3154 (1973).
(34) J. J. Flynn and F. P. Boer, *J. Am. Chem. Soc.*, **91**, 5756 (1969).
(35) D. L. Kepert, *Inorg. Chem.*, **11**, 1561 (1972).
(36) A. Avdeef and J. P. Fackler, Jr., *Inorg. Chem.*, **14**, 2002 (1975).
(37) R. A. D. Wentworth, *Coord. Chem. Rev.*, **9**, 171 (1972).
(38) C. J. Ballhausen, "Introduction to Ligand Field Theory", McGraw-Hill, New York, N.Y., 1962, p 239.
(39) K. Nakamoto and P. J. McCarthy, "Spectroscopy and Structure of Metal Chelate Compounds", Wiley, New York, N.Y., 1968.
(40) C. G. Pierpont and H. H. Downs, *J. Am. Chem. Soc.*, **97**, 2123 (1975).

Metal–Metal Multiple Bonds in Organometallic Compounds. I. (Di-*tert*-butylacetylene)hexacarbonyldiiron and -dicobalt

F. Albert Cotton,* Jackie D. Jamerson, and B. Ray Stults

Contribution from Department of Chemistry, Texas A&M University, College Station, Texas 77843. *Received August 26, 1975*

Abstract: The compound $[(CH_3)_3CC{\equiv}CC(CH_3)_3]Fe_2(CO)_6$ has been prepared and characterized structurally. It consists of two $Fe(CO)_3$ groups joined by a short, 2.316 (1) Å, iron–iron bond which can be formulated as a double bond. The compound forms black crystals belonging to the monoclinic system, space group $P2_1/n$, with unit cell dimensions a = 13.824 (4) Å, b = 9.776 (3) Å, c = 13.826 (5) Å, β = 94.26 (3)°, V = 1863 (1) Å^3, and Z = 4. The structure was solved and refined to final discrepancy indices of R_1 = 0.049 and R_2 = 0.069 using 1767 reflections having $I > 3\sigma(I)$ out of a total of 2442 reflections measured. For comparison, the corresponding cobalt compound, $(t\text{-}BuC_2)Co_2(CO)_6$, was also prepared and its structure determined. This should contain a Co–Co single bond and the Co–Co distance found is 2.463 (1) Å. The cobalt compound forms deep maroon crystals belonging to the triclinic system, space group $P\bar{1}$, with unit cell dimensions a = 8.394 (4) Å, b = 8.491 (6) Å, c = 13.825 (6) Å, α = 88.39 (5)°, β = 94.73 (5)°, γ = 106.86 (4)°, V = 940 (1) Å^3, and Z = 2. The structure was refined to final discrepancy indices of R_1 = 0.038 and R_2 = 0.062, using 2246 reflections with $I > 3\sigma(I)$ out of a total of 2660 reflections measured. The two structures are very similar in most ways (e.g., the C≡C distances are 1.311 (10) and 1.335 (6) Å for the Fe and Co compounds, respectively) but differ in the relative orientations of the CO groups. In the cobalt compound the $Co_2(CO)_6$ group has virtual C_{2v} symmetry whereas in the iron compound one $Fe(CO)_3$ group is rotated by about 60° so that the $Fe_2(CO)_6$ group has only a mirror plane passing through the two iron atoms and two CO groups.

During the last 20 years a variety of compounds have been isolated from the reaction of acetylenes (R_2C_2) and various iron carbonyls.[1] These reactions tend to be complicated producing numerous products whose yields and compositions are dependent upon such things as temperature, reaction time, nature of the R group, etc. In addition, the majority of these complexes contain organic ligands which are no longer simple acetylenes but rather are cyclic derivatives of the acetylene employed. It is not surprising then to discover that only three types of simple acetylene–iron carbonyl complexes have been reported to date: $(R_2C_2)Fe(CO)_4$, R = $SiMe_3$,[1,2] *t*-Bu;[1,3] $(t\text{-}Bu_2C_2)_2Fe_2(CO)_4$;[4] and $(R_2C_2)Fe_2(CO)_6$[5] which appears to be identical in type with those previously formulated by Hubel and co-workers as $(R_2C_2)Fe_2(CO)_7$.[1]

We present here a full account of the synthesis and crystal structure of $(t\text{-}Bu_2C_2)Fe_2(CO)_6$, which was previously the subject of a short communication.[5] In addition, we report the results of a structure determination of the closely related $(t\text{-}Bu_2C_2)Co_2(CO)_6$. The latter study was undertaken because the structure of $(Ph_2C_2)Co_2(CO)_6$[6] had not been accurately determined. The structure of $(t\text{-}Bu_2C_2)Co_2(CO)_6$ was done, rather than a redetermination of the $(Ph_2C_2)Co_2(CO)_6$ structure, so that a very direct comparison with $(t\text{-}Bu_2C_2)Fe_2(CO)_6$ might be made.

Experimental Section

All operations were carried out in an atmosphere of dry nitrogen. Solvents were dried over potassium benzophenone and were distilled under nitrogen just prior to use. Diiron nonacarbonyl was purchased from Pressure Chemical Co., dicobalt octacarbonyl from Strem Chemical Co., and di-*tert*-butylacetylene, $t\text{-}Bu_2C_2$, 98%, from Chemical Samples Co. Infrared spectra were recorded on a Perkin-Elmer 237B spectrometer and were calibrated with polystyrene.

Synthsis of $(t\text{-}Bu_2C_2)Fe_2(CO)_6$. A mixture of 2.34 g (6.43 mmol) of $Fe_2(CO)_9$ and 0.89 g (6.4 mmol) of $t\text{-}Bu_2C_2$ in 40 ml of hexane was stirred at ambient temperature for 24 h. During this time the $Fe_2(CO)_9$ was consumed and the color of the solution became dark green. The reaction solution was filtered and the filtrate was then evaporated to dryness in vacuo at ambient temperature yielding 1.8 g (60%) of crude product. Black crystals of $(t\text{-}Bu_2C_2)Fe_2(CO)_6$ were obtained by recrystallization of the crude product from pentane at −40 °C. Yellow crystals of $(t\text{-}Bu_2C_2)Fe(CO)_4$ were also deposited[3] and were physically separated from the $(t\text{-}Bu_2C_2)Fe_2(CO)_6$ crystals. Ir (hexane): 2050, 2005, 1984, 1973 (sh), and 1968 (sh) cm^{-1}.

Synthesis of $(t\text{-}Bu_2C_2)Co_2(CO)_6$. This compound was prepared by allowing an equimolar mixture of $Co_2(CO)_8$ and $t\text{-}Bu_2C_2$ in hexane to react as previously described.[7,8] The crude product was recrystallized from pentane at −40 °C yielding large, deep maroon crystals. Ir (hexane): 2073, 2035, 2020, 2005, and 1990 cm^{-1}.

X-Ray Data Collection for $(t\text{-}Bu_2C_2)Fe_2(CO)_6$. A black crystal of $(t\text{-}Bu_2C_2)Fe_2(CO)_6$ measuring approximately 0.35 × 0.30 × 0.20 mm was sealed in a glass capillary. All data were collected at 21 ± 2 °C on a Syntex $P\bar{1}$ automated diffractometer using Mo Kα radiation monochromatized with a graphite crystal in the incident beam.

The automatic centering and autoindexing procedures followed have been described.[9] Systematic absences, of $h0l$ ($h + l \neq 2n$) and $0k0$ ($k \neq 2n$), indicated that the space group was $P2_1/n$. The principal crystallographic data are summarized as follows: a = 13.824 (4), b = 9.776 (3), c = 13.826 (5) Å; β = 94.26 (3)°; V = 1863 (1) Å^3; d_{calcd} = 1.49 g/cm^3 for Z = 4 and a molecular weight of 418.02.

A total of 2442 unique reflections with $0° < 2\theta \leq 45°$ were collected using the θ–2θ scan technique, variable scan rates from 4.0